

The structures of magnetic islands formed during collisionless magnetic reconnections in a force-free current sheet

Feibin Fan, Can Huang, Quanming Lu, Jinlin Xie, and Shui Wang

Citation: *Physics of Plasmas* **23**, 112106 (2016); doi: 10.1063/1.4967286

View online: <http://dx.doi.org/10.1063/1.4967286>

View Table of Contents: <http://scitation.aip.org/content/aip/journal/pop/23/11?ver=pdfcov>

Published by the [AIP Publishing](#)

Articles you may be interested in

[A two-fluid study of oblique tearing modes in a force-free current sheet](#)

Phys. Plasmas **23**, 012112 (2016); 10.1063/1.4940945

[The evolution of the ion diffusion region during collisionless magnetic reconnection in a force-free current sheet](#)

Phys. Plasmas **22**, 092110 (2015); 10.1063/1.4930217

[Octupolar out-of-plane magnetic field structure generation during collisionless magnetic reconnection in a stressed X-point collapse](#)

Phys. Plasmas **21**, 060705 (2014); 10.1063/1.4885378

[Current disruption and its spreading in collisionless magnetic reconnection](#)

Phys. Plasmas **20**, 112101 (2013); 10.1063/1.4827828

[Electron scale structures in collisionless magnetic reconnection](#)

Phys. Plasmas **16**, 050704 (2009); 10.1063/1.3134045



COMPLETELY REDESIGNED!

PHYSICS TODAY

Physics Today Buyer's Guide
Search with a purpose.

The structures of magnetic islands formed during collisionless magnetic reconnections in a force-free current sheet

Feibin Fan,^{1,2} Can Huang,^{1,2,a)} Quanming Lu,^{1,2} Jinlin Xie,³ and Shui Wang^{1,2}

¹CAS Key Lab of Geospace Environment, Department of Geophysics and Planetary Science, University of Science and Technology of China, Hefei 230026, China

²Collaborative Innovation Center of Astronautical Science and Technology, Harbin 150001, China

³CAS Key Lab of Geospace Environment, Department of Modern Physics, University of Science and Technology of China, Hefei 230026, China

(Received 24 August 2016; accepted 21 October 2016; published online 8 November 2016)

In this paper, with a two-dimensional particle-in-cell simulation model, we compare the structures of a primary magnetic island to those of a secondary magnetic island, and these islands are formed during collisionless magnetic reconnection in a force-free current sheet. The out-of-plane magnetic field B_y is enhanced in the center of both the primary and secondary islands; however, a quadrupole structure of B_y with a good symmetry may be formed at the ends of the primary island. The in-plane electric field also exists in both the primary and secondary islands. The electric field E_x has a positive value in the left and a negative value in the right of the islands, while the electric field E_z has a positive value in the upper part and a positive value in the lower part of the islands. However, the in-plane electric field exists in the outer part of the primary island, while it exists in the center of the secondary island. *Published by AIP Publishing.*

[<http://dx.doi.org/10.1063/1.4967286>]

I. INTRODUCTION

Magnetic reconnection, as a fundamental physical process in plasmas, rapidly converts magnetic energy into plasma kinetic and thermal energy with topological rearrangement of magnetic field lines.^{1,2} It is believed that magnetic reconnection plays an important role in explaining many explosive phenomena in the solar atmosphere, the earth's magnetosphere, and laboratory plasmas.^{3–6} In collisionless magnetic reconnection, the diffusion region is found to have a multi-scale structure.^{7–12} In the ion diffusion region with the scale below the ion inertial length, the ions are unmagnetized and electrons are frozen in the magnetic field. In the electron diffusion region with the scale below the electron inertial length, both the ions and electrons are unmagnetized. In the ion diffusion region of anti-parallel reconnection, which occurs in a Harris current sheet, the in-plane currents are directed away from the X line along the separatrices and toward the X line along the magnetic field lines just inside the separatrices, and such an in-plane current system results in the quadrupole structure of the out-of-plane magnetic field.^{12–17} However, with the introduction of an initial guide field in a Harris current sheet, the symmetry of the quadrupole structure will become distorted.^{18–20} Recently, magnetic reconnection in a force-free current sheet has been studied, and a distorted quadrupole structure of the out-of-plane magnetic field is at first formed in the ion diffusion region, which is similar to that of a typical guide field reconnection in the Harris current sheet; then, a quadrupole structure of the out-of-plane magnetic field with a good symmetry

emerges in the ion diffusion region, which is similar to that of anti-parallel reconnection in the Harris current sheet.^{21,22}

Magnetic islands, which may be generated via the tearing instability or Kelvin-Helmholtz instability in a current sheet, are considered to enhance not only the reconnection rate but also the efficiency of particle acceleration.^{16,23–25} The structures of the magnetic island formed during multiple X line reconnection in a Harris current sheet have been thoroughly studied with particle-in-cell (PIC) simulations.^{26–29} The out-of-plane magnetic field in the magnetic island formed during anti-parallel reconnection exhibits a symmetric quadrupole structure, and the symmetry will be distorted with the existence of the guide field.³⁰ When the guide field is sufficiently large, the out-of-plane magnetic field is enhanced in the whole magnetic island, while the enhancement is stronger at the edge and a dip is formed at the center of the magnetic island.^{30–32} Lu *et al.*³³ found that the Weibel instability may be unstable in the magnetic island formed during anti-parallel reconnection, where a regular structure with alternate positive and negative values of the out-of-plane magnetic field is generated. Besides the magnetic island formed simultaneously with the appearance of the X line (the primary magnetic island), a secondary magnetic island may also be generated in an extended current sheet around the X line.^{23,30,34} In this paper, with two-dimensional (2-D) PIC simulations, we compare the structures of a primary island with those of a secondary island formed during magnetic reconnection in a force-free current sheet, and the mechanisms for the generation of the magnetic structures are also discussed.

The paper is organized as follows: the 2D PIC simulation model is described in Sec. II, and the simulation results are presented in Sec. III. The summary and discussion are given in Sec. IV.

^{a)}Author to whom correspondence should be addressed. Electronic mail: canhuang@mail.ustc.edu.cn

II. SIMULATION MODEL

In this paper, we use a 2D PIC simulation model to investigate the characteristics of magnetic islands formed during multiple X line magnetic reconnection in a force-free current sheet. In the simulation, the electromagnetic fields are defined on the grids and advanced by solving the Maxwell equations, and the particles are updated by integrating the Newton-Lorentz equations. A force-free current layer is used as the initial condition in the simulation model and the initial magnetic field is given by:

$$\mathbf{B}(z) = B_0 \tanh[z/\delta] \mathbf{e}_x + B_0 \operatorname{sech}[z/\delta] \mathbf{e}_y,$$

where B_0 is the asymptotical magnetic strength. L_z is the length of the computation domain in the z direction. $\delta = 0.5d_i$ is the half-width of the current sheet (here $d_i = c/\omega_{pi}$ is the ion inertial length defined by n_0 , and n_0 is the initial number density). The mass ratio of the ion to the electron is set to be $m_i/m_e = 100$, and the light speed is $c = 20v_A$ (where v_A is the Alfvén speed defined by B_0 and n_0). The parameters are normalized as follows: the spatial coordinate is normalized by d_i , the time is normalized by Ω_i^{-1} (where $\Omega_i = eB_0/m_i$ is the ion gyrofrequency), the magnetic field is normalized by B_0 , the electric field is normalized by B_0V_A , the plasma density is normalized by n_0 , the current is normalized by en_0V_A , and the pressure is normalized by $n_0m_iV_A^2$.

The size of the simulation domain is $L_x \times L_z = 102.4d_i \times 12.8d_i$ with the grid $N_x \times N_z = 2048 \times 256$, so the spatial resolution is $0.05c/\omega_{pi}$ in both the x and z directions. The time step is set to be $\Omega_i \Delta t = 0.001$ (where Ω_i is the ion gyrofrequency). We employ 100 particles per species in each grid, which means that more than 5×10^7 particles per species are used in the whole domain. The periodic boundary conditions are used in the x direction, while in the z direction the ideal conducting boundary conditions are used for electromagnetic fields and the reflected boundary conditions for particles. In this simulation, we introduce an initial flux perturbation for the system to enter the nonlinear stage more quickly.

III. SIMULATION RESULTS

In this paper, a 2D PIC simulation model is employed to investigate the characteristics of magnetic islands formed during multiple X line magnetic reconnection in a force-free current sheet. Figure 1 shows the time evolution of the out-of-plane magnetic field B_y , and in the figure the magnetic field lines are also plotted for reference. With the development of the reconnection, at about $\Omega_i t = 20$ two X lines appear around $x = -25d_i$ and $28d_i$, and a primary magnetic island is formed between the two X lines. The length of the magnetic island shrinks gradually, and their width increases. During such a process, the out-of-plane magnetic field B_y is enhanced in the center of the primary island. With the formation of the primary island, the regions with a negative value of B_y begin to appear at the lower-left and upper-right parts of the island. At about $\Omega_i t = 60$, a quadrupole structure of B_y with a good symmetry, which is detached from the center of the primary island with an enhancement of B_y , is formed at

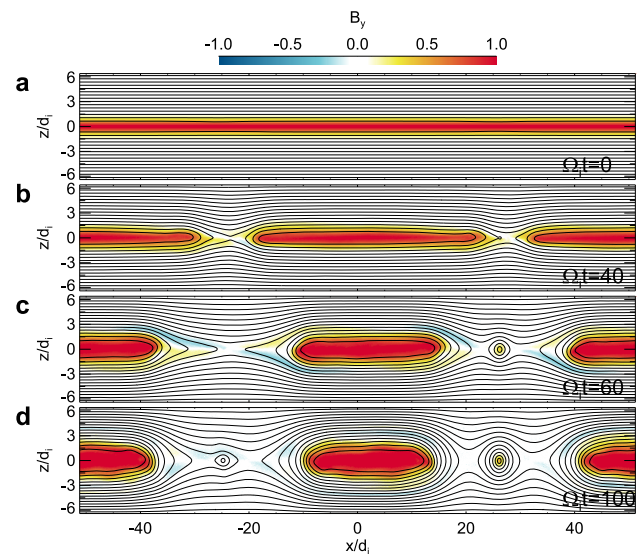


FIG. 1. The time evolution of the out-of-plane magnetic field B_y at (a) $\Omega_i t = 0$, (b) $\Omega_i t = 40$, (c) $\Omega_i t = 60$, and (d) $\Omega_i t = 100$. The in-plane magnetic field lines are also plotted.

the ends of the primary island. Such a quadrupole structure of B_y disappears at about $\Omega_i t = 90$.

Two secondary magnetic islands are also successively generated during the process of magnetic reconnection, and their positions are around $x = -25d_i$ and $26d_i$, respectively. The island around $x = 26d_i$ is formed at about $\Omega_i t = 45$, where the out-of-plane magnetic field is obviously enhanced. The island around $x = -25d_i$ is formed at about $\Omega_i t = 85$, and no obvious enhancement of the out-of-plane magnetic field is found.

In order to study the generation mechanism of the out-of-plane magnetic field B_y in these magnetic islands, in Figure 2, we plot the parallel electron current $J_{e\parallel} = \mathbf{J}_e \cdot \mathbf{B}'/B'$ (where $\mathbf{B}' = B_x \mathbf{e}_x + B_z \mathbf{e}_z$ is the in-plane magnetic field), the ion current $J_{i\parallel} = \mathbf{J}_i \cdot \mathbf{B}'/B'$, and the total current $J_{\parallel} = J_{e\parallel} + J_{i\parallel}$. According to Ampère's Law and $\partial/\partial y = 0$, we can derive $-\partial B_y/\partial z = J_x$ and $\partial B_y/\partial x = J_z$. B_y is only related to the in-plane currents. In the whole paper "||" means parallel to the in-plane magnetic field. Figure 3(a) shows the cut of the parallel current along $x = 26.2d_i$ at $\Omega_i t = 60$, which crosses the center of the secondary island. It can be found that the parallel current in the outer part is stronger than that in the inner part, which leads to the enhancement of the out-of-plane magnetic field in the center of the secondary island. In the primary magnetic island, similarly, the total current sheet is also along the magnetic field, and the parallel current in the outer part is stronger than that in the inner part. We can observe the enhancement of the out-of-plane magnetic field in the center of the primary island. However, around $\Omega_i t = 60$, at the two ends of the primary island, the parallel current, which is contributed mainly by the electron current, is away from the X line along the separatrices, while it is directed toward the X line along the in-plane magnetic field just inside the separatrices. This can be demonstrated more clearly in Figure 3(b), which shows the cut of the parallel current along $x = 19d_i$ at $\Omega_i t = 60$, which crosses one end of the primary island. Such a distribution of

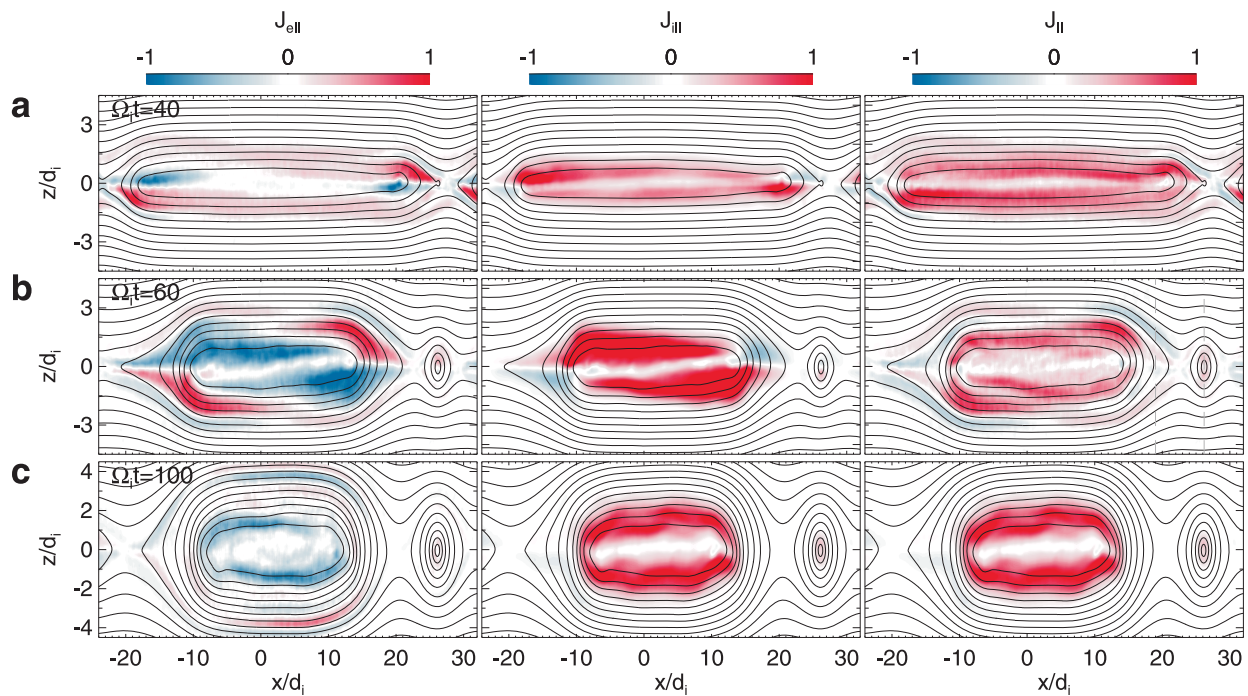


FIG. 2. The contours of the parallel electron current $J_{e||} = \mathbf{J}_e \cdot \mathbf{B}'/B'$ (where $\mathbf{B}' = B_x \mathbf{e}_x + B_z \mathbf{e}_z$ is the in-plane magnetic field), parallel ion current $J_{i||} = \mathbf{J}_i \cdot \mathbf{B}'/B'$, and parallel total current $J_{||} = J_{e||} + J_{i||}$ at (a) $\Omega_i t = 40$, (b) $\Omega_i t = 60$, and (c) $\Omega_i t = 100$. The in-plane magnetic field lines are also plotted.

the parallel current results in a quadrupole structure of the out-of-plane magnetic field B_y at the ends of the primary island. Such a pattern of the parallel current at the ends of the primary island disappears at about $\Omega_i t = 50$.

Figures 4 and 5 plot the distribution of the electron number density n_e and the amplitude of the Ampere force acting on the plasma element $|\mathbf{J} \times \mathbf{B}|$ in the primary and secondary islands, respectively. The amplitude of $|\mathbf{J} \times \mathbf{B}|$ represents the level of the violation of the force-free condition, which is

violated in both the primary and secondary islands. In the primary magnetic island, the region, where the force-free condition is violated, forms a ring distribution, and the enhancement of the electron density also occurs in a ring

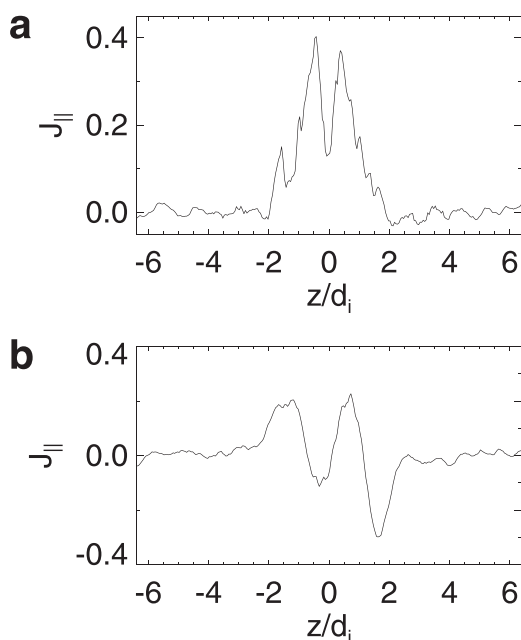


FIG. 3. The profile of the parallel total current $J_{||}$ along the lines (a) $x = 26.2d_i$ and (b) $x = 19d_i$ at $\Omega_i t = 60$.

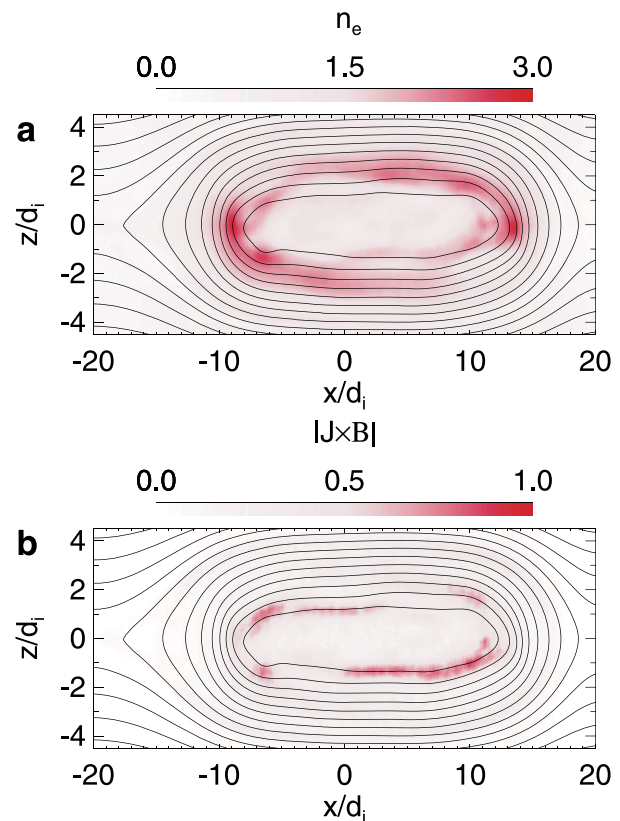


FIG. 4. The contours of electron density n_e and $|\mathbf{J} \times \mathbf{B}|$ of the primary magnetic island at $\Omega_i t = 100$. The in-plane magnetic field lines are also presented.

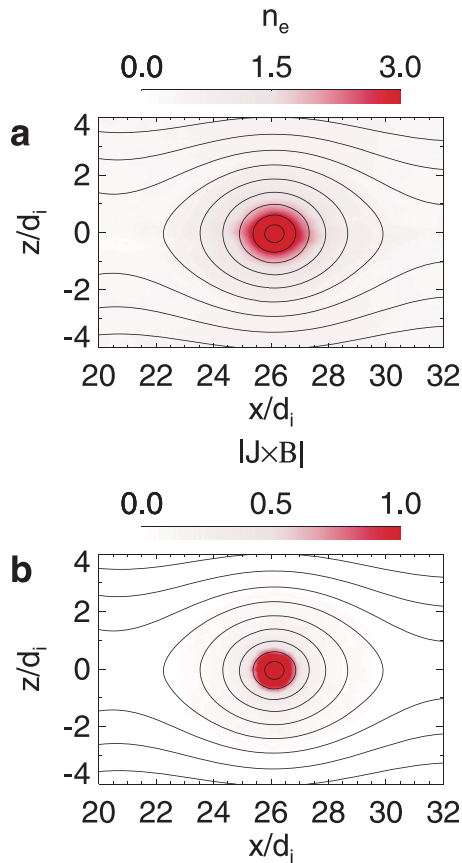


FIG. 5. The contours of electron density n_e and $|\mathbf{J} \times \mathbf{B}|$ of the secondary magnetic island around $x = 26d_i$ at $\Omega_i t = 100$. The in-plane magnetic field lines are also presented.

distribution. In the center of the primary island, we cannot find obvious enhancement of the electron density, and the force-free condition is kept. In the secondary island, both the violation of the force-free condition and the enhancement of the electron density occur in the center of the island.

According to the general Ohm's law, the electric field force is balanced by the pressure gradient, electromagnetic force, and inertia force in the plasma. Note that the inertia term is close to zero in the islands, so it is neglected here. Figures 6 and 7 show (a) the electric fields E_x and E_z , (b) the contributions from the off-diagonal electron pressure tensor term to the electric field $(-\nabla \cdot \mathbf{P}/en_e)_x$ and $(-\nabla \cdot \mathbf{P}/en_e)_z$, and (c) the contributions from the electromotive force term to the electric field $(-\mathbf{V}_e \times \mathbf{B})_x$ and $(-\mathbf{V}_e \times \mathbf{B})_z$, in the primary and secondary islands, respectively. The electron inertia term is not shown here, because it is smaller and negligible. In both the primary and secondary islands, the in-plane electric fields E_x and E_z are dominated by the electromotive force term. The electric field E_x has a positive value in the left of the islands, and it is negative in the right. The electric field E_z has a positive value in the upper part of the islands, and it is positive in the lower part. However, the in-plane electric field exists in the outer part of the primary island, while it exists in the center of the secondary island.

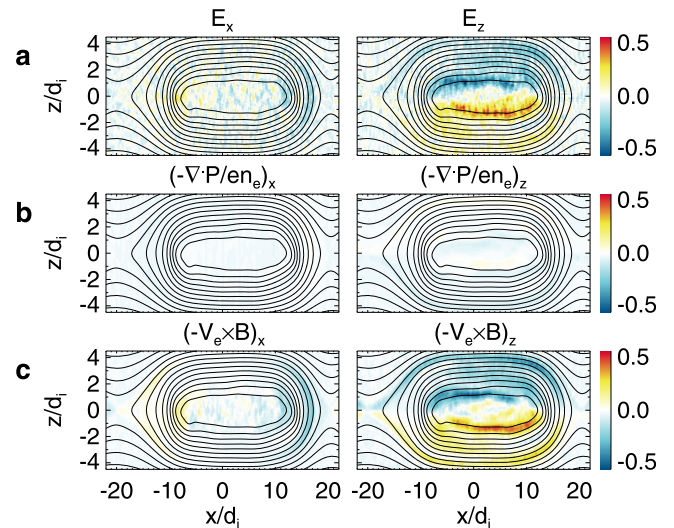


FIG. 6. The x and z components of (a) \mathbf{E} , (b) $-\nabla \cdot \mathbf{P}/en_e$, and (c) $-\mathbf{V}_e \times \mathbf{B}$ of the primary magnetic island at $\Omega_i t = 100$. The in-plane magnetic field lines are also presented.

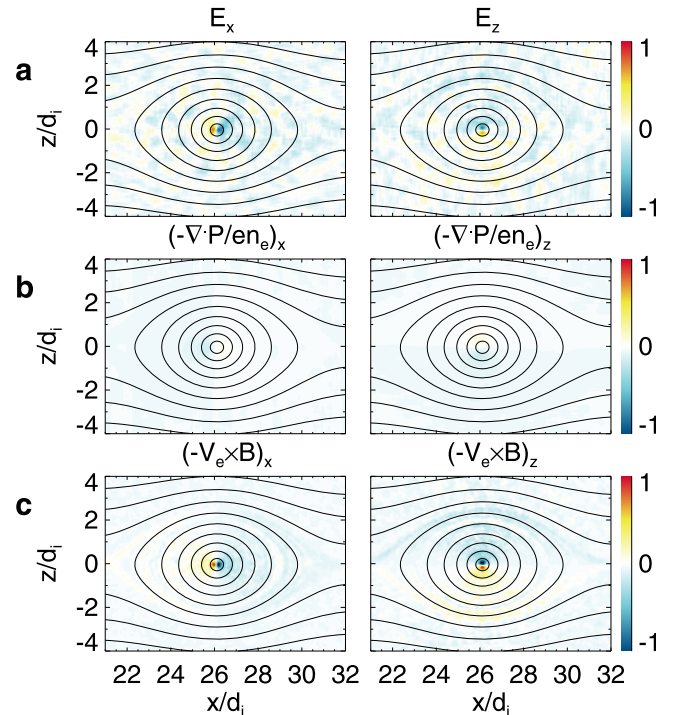


FIG. 7. The x and z components of (a) \mathbf{E} , (b) $-\nabla \cdot \mathbf{P}/en_e$, and (c) $-\mathbf{V}_e \times \mathbf{B}$ of the secondary magnetic island around $x = 26d_i$ at $\Omega_i t = 100$. The in-plane magnetic field lines are also presented.

IV. CONCLUSIONS AND DISCUSSION

Recently, an extended electron diffusion region is found to be unstable plasmoid instability^{35,36} and secondary islands may be formed during magnetic reconnection.^{23,30} In this paper, we use a 2D PIC simulation model to compare the characteristics of both the primary and secondary islands formed during magnetic reconnections in a force-free current sheet. The out-of-plane magnetic field B_y can be enhanced in the center of both the primary and secondary islands. However, the enhancement of B_y in a secondary island

depends on the time when the island is formed. The out-of-plane magnetic field B_y will be gradually pushed away from the electron diffusion region during magnetic reconnection. If the secondary island is formed early when the out-of-plane magnetic field is still sufficiently strong in the electron diffusion region, we can observe obvious enhancement of B_y in the secondary island. When the secondary island is formed later after the out-of-plane magnetic field is almost pushed away from the electron diffusion region, there is no obvious enhancement of B_y in the secondary island. Also, a quadrupole structure of B_y with a good symmetry may be formed at the ends of a primary island. The characteristics of the primary island formed during magnetic reconnection in a force-free current sheet are different from those in a Harris current sheet. A symmetric quadrupole structure of the out-of-plane magnetic field is formed in a primary island generated during magnetic reconnection in a Harris current sheet without a guide field, and the introduction of a guide field can distort the symmetry of the quadrupole structure of the out-of-plane magnetic field in the primary island. When the guide field is sufficiently strong, the out-of-plane magnetic field is enhanced inside the primary island with a dip in the center of the island.²⁸ The out-of-plane magnetic field can be enhanced only in the center of the secondary island formed during magnetic reconnection in a Harris current sheet with a guide field.³⁷

The force-free condition can be violated in both the primary and secondary islands. The violation of the force-free condition occurs in the center of the secondary island, while in the primary island it occurs in the region with a ring distribution. Also, the in-plane electric field exists in the region with a ring distribution in the primary island, while it exists in the center of the secondary island. The electric field E_x has a positive value in the left and a negative value in the right of the islands, while the electric field E_z has a positive value in the upper part and a positive value in the lower part of the islands. The characteristics of the in-plane electric field of both the primary and secondary islands formed in a force-free current sheet are similar to those formed in a Harris current sheet.^{29,38}

ACKNOWLEDGMENTS

This research was supported by the National Science Foundation of China, Grant Nos. 41331067, 41474125, 41527804, 11220101002, and 41421063, 973 Program (2013CBA01503).

¹V. M. Vasyliunas, *Rev. Geophys. Space Phys.* **13**, 303, doi:10.1029/RG013i001p00303 (1975).

²E. Priest and T. Forbes, *Magnetic Reconnection: MHD Theory and Applications* (Cambridge University Press, Cambridge, 2000).

³R. G. Giovanelli, *Nature (London)* **158**, 81 (1946).

⁴D. N. Baker, T. I. Pulkkinen, V. Angelopoulos, W. Baumjohann, and R. L. McPherron, *J. Geophys. Res.* **101**(A6), 12975, doi:10.1029/95JA03753 (1996).

⁵H. Ji, M. Yamada, S. Hsu, and K. Russell, *Phys. Rev. Lett.* **80**(15), 3256 (1998).

⁶R. S. Wang, Q. M. Lu, A. M. Du, and S. Wang, *Phys. Rev. Lett.* **104**, 175003 (2010).

⁷B. U. Ö. Sonnerup, "Magnetic field reconnection," in *Solar System Plasma Physics*, edited by L. J. Lanzerotti, C. F. Kennel, and E. N. Parker (North-Holland, New York, 1979), Vol. 3, p. 46.

⁸T. Terasawa, *Geophys. Res. Lett.* **10**, 475, doi:10.1029/GL010i006p00475 (1983).

⁹J. Birn, J. F. Drake, M. A. Shay, B. N. Rogers, R. E. Denton, M. Hesse, M. Kuznetsova, Z. W. Ma, A. Bhattacharjee, A. Otto, and P. L. Pritchett, *J. Geophys. Res.* **106**, 3715, doi:10.1029/1999JA900449 (2001).

¹⁰M. A. Shay, J. F. Drake, B. N. Rogers, and R. E. Denton, *J. Geophys. Res.* **106**, 3759, doi:10.1029/1999JA001007 (2001).

¹¹R. S. Wang, Q. M. Lu, C. Huang, and S. Wang, *J. Geophys. Res.* **115**, A01209, doi:10.1029/2009JA014553 (2010).

¹²Q. M. Lu, C. Huang, J. L. Xie, R. S. Wang, M. Y. Wu, A. Vaivads, and S. Wang, *J. Geophys. Res.* **115**, A11208, doi:10.1029/2010JA015713 (2010).

¹³P. L. Pritchett, *J. Geophys. Res.* **106**, 3783, doi:10.1029/1999JA001006 (2001).

¹⁴T. Nagai, I. Shinohara, M. Fujimoto, M. Hoshino, Y. Saito, S. Machida, and T. Mukai, *J. Geophys. Res.* **106**, 25929, doi:10.1029/2001JA900038 (2001).

¹⁵T. Nagai, I. Shinohara, M. Fujimoto, S. Machida, R. Nakamura, Y. Saito, and T. Mukai, *J. Geophys. Res.* **108**, 1357, doi:10.1029/2003JA009900 (2003).

¹⁶X. R. Fu, Q. M. Lu, and S. Wang, *Phys. Plasmas*, **13**, 012309 (2006).

¹⁷S. Lu, Q. M. Lu, Y. Cao, C. Huang, J. L. Xie, and S. Wang, *Chin. Sci. Bull.* **56**, 48 (2011).

¹⁸B. N. Rogers, R. E. Denton, and J. F. Drake, *J. Geophys. Res.* **108**, 1111, doi:10.1029/2002JA009699 (2003).

¹⁹P. L. Pritchett and F. V. Coroniti, *J. Geophys. Res.* **109**, A01220, doi:10.1029/2003JA009999 (2004).

²⁰C. Huang, Q. M. Lu, and S. Wang, *Phys. Plasmas*, **17**, 072306 (2010).

²¹F. S. Zhou, C. Huang, Q. M. Lu, J. L. Xie, and S. Wang, *Phys. Plasmas*, **22**, 092110 (2015).

²²F. Wilson, T. Neukirch, M. Hesse, M. G. Harrison, and C. R. Stark, *Phys. Plasmas*, **23**, 032302 (2016).

²³W. Daughton, J. Scudder, and H. Karimabadi, *Phys. Plasmas*, **13**, 072101 (2006).

²⁴W. Daughton, V. Roytershteyn, H. Karimabadi, L. Yin, B. J. Albright, B. Bergen, and K. J. Bowers, *Nat. Phys.* **7**, 539 (2011).

²⁵C. Huang, Q. M. Lu, F. Guo, M. Y. Wu, A. M. Du, and S. Wang, *Geophys. Res. Lett.* **42**, 7282, doi:10.1002/2015GL065690 (2015).

²⁶H. Karimabadi, D. Krauss-Varban, N. Omidi, and H. X. Vu, *J. Geophys. Res.* **104**, 12313, doi:10.1029/1999JA900089 (1999).

²⁷H. Karimabadi, J. D. Huba, D. Krauss-Varban, and N. Omidi, *Geophys. Res. Lett.* **31**, L07806, doi:10.1029/2004GL019553 (2004).

²⁸C. Huang, Q. M. Lu, H. Zhang, M. Y. Wu, Q. L. Dong, S. Lu, and S. Wang, *Phys. Plasmas*, **19**, 042111 (2012).

²⁹S. Y. Huang, M. Zhou, Z. G. Yuan, X. H. Deng, F. Sahraoui, Y. Pang, and S. Fu, *J. Geophys. Res.* **119**, 7402, doi:10.1002/2014JA020054 (2014).

³⁰J. F. Drake, M. Swisdak, K. M. Schoeffler, B. N. Rogers, and S. Kobayashi, *Geophys. Res. Lett.* **33**, L13105, doi:10.1029/2006GL025957 (2006).

³¹L. J. Chen, A. Bhattacharjee, P. A. Puhl-Quinn, H. Yang, N. Bessho, S. Imada, S. Muehlbacher, P. W. Daly, B. Lefebvre, Y. Khotyaintsev, A. Vaivads, A. Fazakerley, and E. Georgescu, *Nat. Phys.* **4**, 19 (2008).

³²C. Huang, Q. M. Lu, S. Lu, P. R. Wang, and S. Wang, *J. Geophys. Res.* **119**, 798, doi:10.1002/2013JA019249 (2014).

³³S. Lu, Q. M. Lu, X. Shao, H. Y. Peter, and S. Wang, *Phys. Plasmas*, **18**, 072105 (2011).

³⁴J. P. Eastwood, T.-D. Phan, F. S. Mozer, M. A. Shay, M. Fujimoto, A. Retino, M. Hesse, A. Balogh, E. A. Lucek, and I. Dandouras, *J. Geophys. Res.* **112**, A06235, doi:10.1029/2006JA012158 (2007).

³⁵A. Bhattacharjee, Y. M. Huang, H. Yang, and B. Rogers, *Phys. Plasmas*, **16**, 112102 (2009).

³⁶Y. M. Huang and A. Bhattacharjee, *Astrophys. J.* **818**, 20 (2016).

³⁷C. Huang, Q. M. Lu, Z. Yang, M. Y. Wu, Q. Dong, and S. Wang, *Nonlinear Processes Geophys.* **18**, 727 (2011).

³⁸M. Zhou, X. H. Deng, and S. Y. Huang, *Phys. Plasmas*, **19**, 042902 (2012).